Wang *et al.*
Journal of Engineering and Applied Science (2022) 69:84
https://doi.org/10.1186/s44147-022-00135-y

Journal of Engineering and Applied Science

RESEARCH Open Access

Design and flow field analysis of impregnated diamond bit for seafloor drill in soft-hard interlaced strata

Jialiang Wang[1,2,3*], Chen Chen[1,3], Dilei Qian[1,3], Fenfei Peng[1,3], Mengfei Yu[1,3], Yang Sun[1,3] and Deping Peng[1,3,4]

*Correspondence:
Jialiangwang2019@163.com

[1] National Local Joint Engineering Laboratory of Marine Mineral Resources Exploration Equipment and Safety Technology, Hunan University of Science and Technology, Xiangtan 411201, China
[2] Key Laboratory of Metallogenic Prediction of Nonferrous Metals and Geological Environment Monitoring, Central South University, Ministry of Education, Changsha, China
[3] School of Mechanical Engineering, Hunan University of Science and Technology, Xiangtan 411201, China
[4] Xiangtan Huajin Heavy Equipment, Co., Ltd., Shaoshan 411300, China

Abstract

According to the seafloor drill working conditions and the complex formation characteristics of the seafloor, this paper aims to improve the adaptability of the diamond bit to the formation and the coring quality. The cutter tooth design scheme of the impregnated diamond bit is proposed, and Fluent analyzes the flow field of drilling fluid at the bottom hole. The results show that the cone cutting tooth bit with the primary and assistant nozzles can directly avoid 85.33% drilling fluid flushing core and reduce the disturbance of drilling fluid to the core samples. The water passage structure of the bit is reasonable, and the upward return velocity of the drilling fluid can be stabilized between 0.7 and 1.8 m/s, which meets the requirements of the upward return of cuttings in seabed strata, and has a good hole wall protection performance. Based on the bottom-jet diamond bit, the assistant nozzles are added. The drilling fluid of the assistant nozzles can better cover the bit crown, conductive to cooling the bit crown. The drilling fluid of the main nozzles can timely up-return along the outer annulus hole wall, conducive to the up-return of the cuttings with drilling fluid. This study can extend existing designs of a seafloor coring bits and bottom hole flow field analysis methods.

Keywords: Marine exploration, Diamond bit, Flow field characteristics, Wireline coring, Complex formation drilling

Introduction

With the accelerated pace of marine exploration and development, deep seabed drilling sampling is the premise of marine geological research, seabed mineral resources exploration, and marine engineering construction survey. It is important to obtain the core samples' high quality and recovery percent [6, 17]. Therefore, the related research work has become a recent research focus. Obtaining core samples directly from the deep seafloor by drilling technology is a direct method to evaluate the reserves of seafloor resources. In order to obtain the core effectively, diamond bits must have excellent performance [8, 11, 28]. Offshore drilling is mainly divided into two operation modes: drilling ship sampling and seafloor drill sampling, as shown in Fig. 1 [13, 15]. Seafloor drills referred to a rig directly launched from the mother ship to the seabed by armored cable

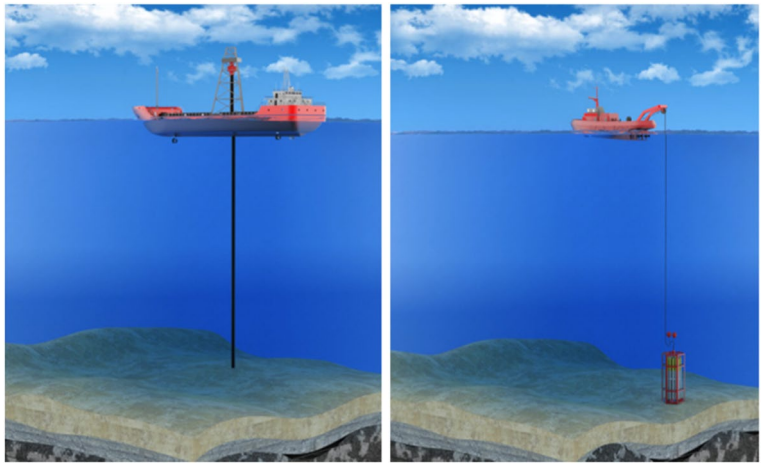

Fig. 1 The main methods used for seafloor coring [13, 15]

and operated on the mother ship deck by remote control. Compared with drilling ships, it provides a feasible technical way for strategic mineral resources and military geological exploration in some particular sea areas and polar sea areas. The seafloor drill has advantages in cost, efficiency, coring quality, convenience, and flexibility in seabed geological coring drilling in a depth of 4000–5000 m and strata of 200–300 m [10, 12].

Interlaced variation of soft and hard strata within 200 m of the seabed are sediments, unconsolidated flow sand, and hard thin layer rocks [2, 25]. Due to the weak ability to resist drilling fluid flushing, low core recovery percent and large disturbance of core samples often occur during drilling. In addition, compared with the drilling ship, there are still the following working condition differences when using the seafloor drill: (1) Because of the small tonnage and low dynamic positioning level of the mother ship carrying the seafloor drill, the seafloor drill has stricter requirements on the working sea conditions. Rigs are usually required to have rapid drilling capacity to reduce the risk of rigs being unable to safely and normally recover due to changes in sea conditions [3]. (2) It is difficult to replace the bit after the bit wear failure, and it is not convenient to select the bit according to the formation conditions [19]. (3) Seawater is usually directly used as drilling fluid in seafloor drills, and its carrying cuttings' ability, wall protection performance, and cooling effect are lower than mud drilling fluid, the potential risks of abnormal wear of matrix, and burning of bit increase [1, 4].

Therefore, it is indispensable to design and optimize the structural parameters of a diamond bit according to the characteristics of seabed strata and the working conditions of seafloor drills. Scouring disturbance of drilling fluid on core samples during drilling is the main factor affecting the sample quality and core recovery percent [24, 27]. A reasonable design of cutting tooth structure of diamond bit to change the flow path of drilling fluid is an effective means to improve coring quality [14, 16, 21]. In addition, the structure of cutting teeth is also an essential factor affecting the drilling efficiency and service life of diamond bits. Based on the fluid dynamics theory, this paper conducts the simulation analysis of the water passage system of the diamond bit. The effect of drilling

fluid flow direction on core recovery by analyzing the velocity contour, pressure contour, and flow trajectory of drilling fluid and combining it with the field test. This research can provide theoretical support and scientific criteria for the optimization strategy of cutting teeth of diamond bits and the quality prediction of core samples, conducive to improving the drilling efficiency and operational reliability of seafloor drills in complex seafloor strata.

Methods

Design of bit parameter scheme

The parameter design of diamond bit usually includes four aspects: matrix formula, diamond parameters, cutting tooth structure, and water passage system. The selected matrix formula is the WC skeleton material commonly used to design impregnated diamond bits. The formula system has better hardness and strength, which is beneficial to ensure the working life [18]. The seafloor within 200-m depth is mainly composed of sediments, supplemented by a hard thin rock, and its rock drillability grade is usually low. Therefore, the rock-breaking efficiency of the bit is improved by increasing the diamond diameter. The diamond particle size is 30/35 mesh, and the volume concentration is 55% [10]. In addition, to promote the cutting edge of the diamond, the hard, brittle SiC particles with an average particle size of 425 μm and a volume concentration of 15% were added to the matrix in this design. The matrix hardness is HRC 25, the cutting teeth numbers are 7, and the waterway numbers are 7.

The cutting tooth structure is an essential factor affecting the drilling efficiency and coring quality. The seafloor strata are changeable due to a series of geological effects. In vertical drilling, multiple strata may occur alternately, called the seafloor complex strata. In order to improve the drilling efficiency of the bit and prevent borehole deviation during the drilling in seafloor complex strata, the cone-tooth structure can increase the centering effect and crown pressure of the bit, and the cutting tooth of the bit is designed as the cone-tooth structure [25]. In order to improve the working life, the working layer height of the bit body, namely the grinding height, is increased to 12 mm. In order to avoid the risk of premature failure of the bit due to excessive wear of the inner and outer diameters, diamond polycrystalline with a double-layer arrangement is selected as the gauge protection material. Conventional water passage diamond bits do not have nozzles, and all drilling fluids flush cores directly from the clearance between the core lifter seat and the bit, as shown in Fig. 2a. Compared with the conventional water passage diamond bit, most of the drilling fluid of the bottom-jet diamond bit flows through the nozzles to avoid direct flushing core, as shown in Fig. 2b. The main waterways are evenly arranged at the bottom of the nozzles, and the diameter of the nozzles is 5 mm, to avoid direct erosion of the core by changing the flow direction of the drilling fluid. Considering that the viscosity of seawater drilling fluid is lower than that of the mud drilling fluid, and its ability to carry the cuttings is weak, it is easy to cause the accumulation of the cuttings at the bottom hole to be ineffective in cooling the crown. In this design, the assistant nozzles are set on the side of the cutting tooth crown near the bit outer wall, and the diameter of the nozzles is 5 mm. The designed bit is shown in Fig. 3.

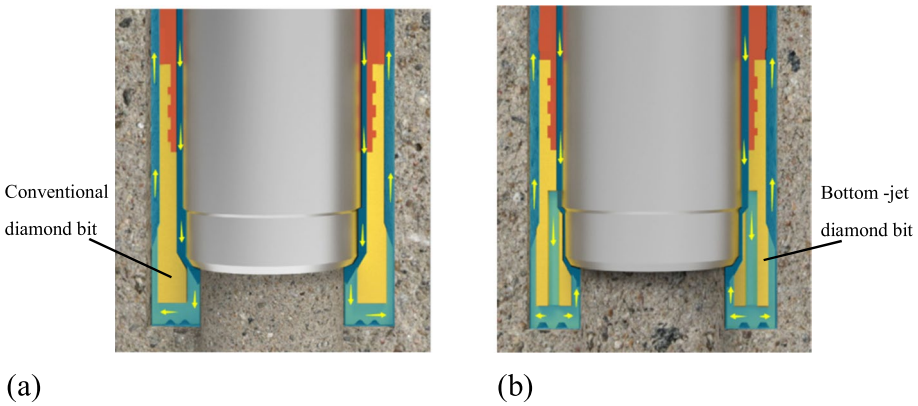

Fig. 2 Difference of water passage between two diamond bits. **a** Conventional water passage diamond bit. **b** Bottom-jet water passage diamond bit

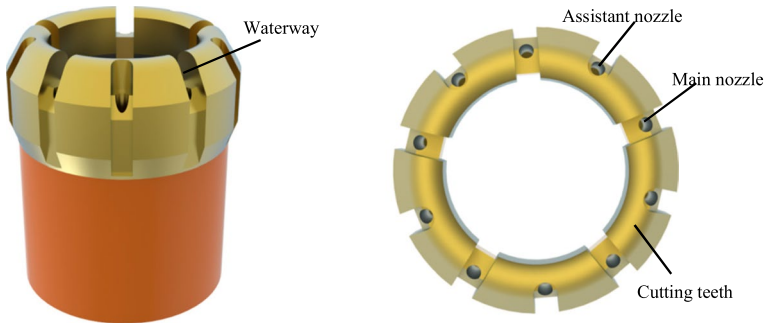

Fig. 3 Diamond bit model diagram

Model establishment and mesh division

Combined with the drilling tool sub-assembly, as shown in Fig. 4, the established water passage system includes six parts [22]. The numerical simulation model is the fluid domain after Boolean operation of six parts: diamond bit, core lifter, core lifter seat, core, hole wall, and stop ring. The simplified model is shown in Fig. 5. The model is divided into unstructured grids by the ICEM CFD module in ANSYS software. Since the cutting tooth structure of the bit in this model is conical and there are many water holes, it increases the difficulty of generating unstructured mesh. Therefore, the model is automatically generated using the octree algorithm to improve the reliability of the results [20]. Volume meshing parameters mainly adopt tetrahedral mixed mesh types. The total mesh numbers in this model are about 13 million, and the mesh smoothing function of CFD is used to smooth the mesh to improve the mesh quality.

Boundary conditions

According to the previous literature, cuttings have little effect on the simulation results in drilling simulation, so the influence of cuttings generated in actual drilling and possible rock particles on the convective field performance is not considered in

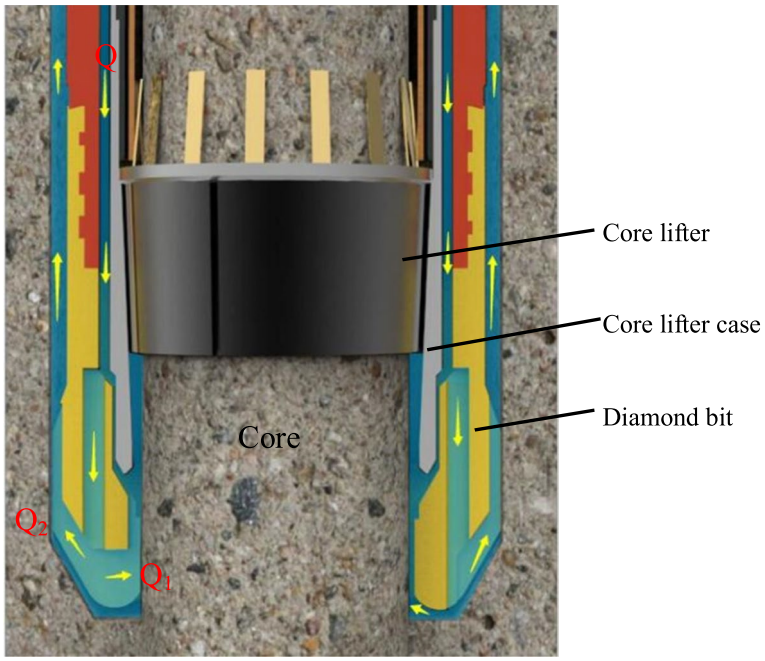

Fig. 4 Drilling tool sub-assembly water passage system

the simulation process [5, 23]. In this simulation, the drilling fluid is seawater, and the density is 1.03×10^3 kg/m^3. According to the core drilling technical regulations of geological survey, the drilling fluid pump displacement is set as 80 L/min. This simulation is set as a mass flow inlet 2; that is, the flow rate of the annular clearance between the bit and the core lifter seat is 1.36×103 kg/m^3. There are two pressure outlets: the annular clearance between the hole wall and the bit 1 and the annular clearance between the core lifter seat and the core 3, and the outlet boundary conditions are 89,000 pa. Other boundaries are set as smooth wall as shown in Fig. 5.

Calculation method

ANSYS Fluent 18.0 carries out the simulation analysis of the water passage system. The SIMPLEC coupling calculation of pressure and velocity can improve the calculation speed, and the convergence accuracy is set to 10^{-5}. The standard K-Epsilon turbulence two-equation model calculates the whole flow channel in this simulation. The time step is set to 500 steps. The required convergence accuracy can be achieved [26].

Results and discussion

Waterproof effect of diamond bit

The total flow rate of the drilling fluid shown in Fig. 4 between the annular clearance between the core lifter seat and the bit is Q. The drilling fluid is divided into two parts when it goes down to the water separation port, one part of which flows to the core. The other part of the drilling fluid is divided into two strands after hitting the bottom hole. One strand of drilling fluid returns along the hole wall, and its flow rate is Q_1. The other strand of drilling fluid combines with the drilling fluid flowing towards the core, and its flow rate is Q_2. According to the flow conservation law, $Q1$

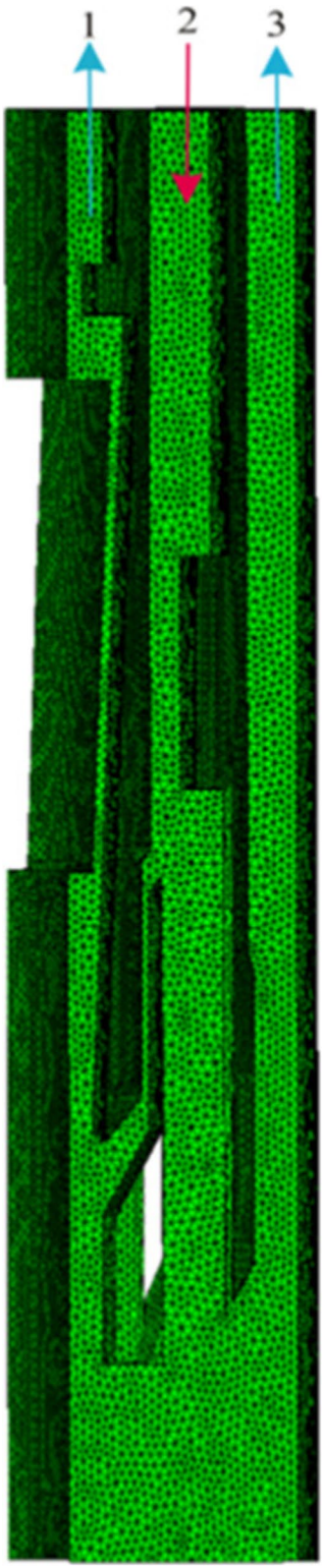

Fig. 5 Water passage mesh model

and $Q2$ are equal to the total flow Q of drilling fluid. The waterproof effect of the bit during drilling is an important factor affecting core recovery. If the flow rate of high-pressure drilling fluid flowing to the core direction is too large (flow rate Q_2), it is easy to aggravate the erosion degree of core samples, resulting in core breakage and collapse, which leads to a decrease in core recovery. In order to scientifically describe the results of simulation data, the ratio method commonly used in engineering applications is used to analyze the waterproof effect of bit. The ratio of outlet flow to total flow is used to evaluate the water insulation effect of bit. As shown in Fig. 5, Q_2 represents the flow rate of drilling fluid at outlet 1 (upward return flow rate), Q_1 represents the flow rate of drilling fluid at outlet 3 (flow to the core), and Q represents the flow rate of drilling fluid at inlet 2 (total flow rate). If the Q_2/Q ratio is small, it shows that the waterproof effect is good and vice versa. Table 1 shows that the designed bit cutting tooth structure can avoid 85.33% drilling fluid flushing core.

Velocity vector analysis of drilling fluid in the bottom hole

Figure 6 is a velocity vector diagram of drilling fluid at the bottom hole cross-section. It can be seen from Fig. 6 that after the drilling, the fluid flows out from the main nozzle 1 of the bit, a part of the drilling fluid returns directly along the hole wall, and the remaining part is two strands. Most of the fluid returns along the hole wall clearance, and a small part forms a vortex near the hole wall. The other part collects at the bottom crown with the drilling fluid from the assistant nozzle 2 and forms a vortex. The proper swirling form is beneficial to improve the carrying cuttings' ability. It can also be seen from Fig. 6 that the drilling fluid flowing from the assistant nozzle completely covers the bottom crown of the bit, which is conducive to avoiding the drill burning accident due to the cooling of the central part of the cutting tooth.

Table 1 Flow rate ratio of the model

Q_1(L/min)	Q_1/Q(%)	Q_2(L/min)	Q_2/Q(%)	Q(L/min)
68.176	85.22	11.824	14.78	80

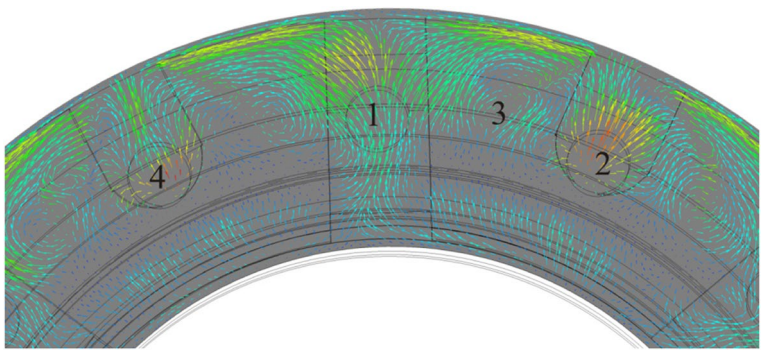

Fig. 6 Bottom nozzles vector diagram. 1 Main nozzle, 2 right assistant nozzle, 3 cutting teeth, and 4 left assistant nozzle

Velocity vector diagram analysis of drilling fluid at nozzle cross-section

Figure 7 is the velocity vector diagram of drilling fluid in the main and assistant nozzle cross-section. It can be seen from Fig. 7a that after the drilling fluid flowed to region 1, most of it went down the nozzle B and outflow from C, and a small part went down the clearance between the core and the core lifter seat along with A. The drilling fluid flow along the clearance between the core and the core lifter seat at A is few, and the velocity is less than 0.6m/s, which has slight flushing to the core. A part of the drilling fluid running under the nozzle at B generates a levorotation vortex along the hole wall after impacting the bottom hole, which improves the cuttings carrying ability of the drilling fluid and avoids the repeated wear of the matrix due to excessive residual cuttings at the bottom hole. The other part of the drilling fluid diffuses along with the bottom crown of the bit and converges with the drilling fluid flowing out of D and generates a dextrorotation vortex at the bottom hole, which is conducive to improving the flow performance of the drilling fluid at the bottom crown of the bit.

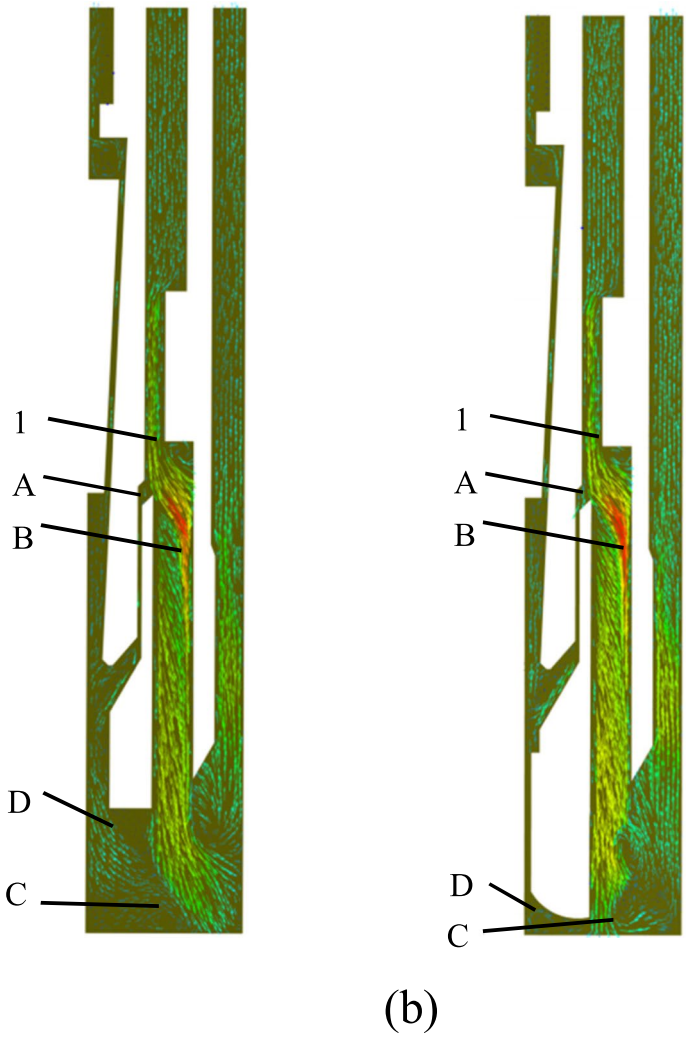

Fig. 7 Speed vector cross-section of nozzles. **a** Main nozzles cross-section. **b** Assistant nozzles cross-section

It can be seen from Fig. 7b that the flow trajectory of the drilling fluid at the 1 region is similar to that of the main nozzle cross-section. However, unlike the velocity vector diagram at the cross-section of the main nozzle, most of the drilling fluid flows along the outer diameter direction of the cutting tooth after the drilling fluid moves under the nozzle at B in the cross-section of the assistant nozzle and outflows from C. Only a tiny part flows along the inner diameter of the cutting tooth and converges with the drilling fluid flowing out at D. The above phenomenon may have the following two reasons: on the one hand, the main and assistant waterway in the outlet structure differences. The assistant waterway is located in the middle of the cutting tooth. The drilling fluid flowing from the assistant nozzle is easily blocked by the cutting tooth, forcing most of it to flow to both sides along the center of the cutting tooth, thereby reducing the flow to the inner diameter of the bit. On the other hand, because the drilling fluid is affected by the sidewall of the cutting tooth at the assistant nozzle outlet, the flow velocity near the sidewall is reduced. There is a flow velocity difference between the drilling fluid at the outlet, which makes the flow rate of the near sidewall flowing along the inner diameter of the cutting tooth small, and the flow rate of the outer diameter of the cutting tooth large, thus forming different flow trajectories. A large amount of drilling fluid flowing along the outer diameter is conducive to taking away the heat generated by the cutting tooth's high-speed rotation and improving the cutting tooth's cooling performance. Combined with the observation in Figs. 6 and 7, it is found that the drilling fluid streamline of the assistant nozzle can better cover the crown, which will be conducive to cooling the bit. In contrast, the drilling fluid streamline of the main nozzle can timely return along the outer ring hole wall, which will be conducive to the return of cuttings with drilling fluid.

Pressure contour analysis of drilling fluid in nozzle cross-section

Figure 8 shows the drilling fluid's pressure contour in the nozzles' cross-section. It can be seen from Fig. 8 that the pressure of drilling fluid at the inlet of main and assistant nozzles is 914,000 Pa, the pressure at the outlet is 0.88 Mpa, and the pressure loss in the process of drilling fluid flow is about 34,000 Pa.

It can be seen from Fig. 8a that the maximum pressure area of the pressure contour of the drilling fluid at the cross-section of the main nozzle appears at the inlet, and the pressure drops to 905,000 Pa when the drilling fluid flows from the region 1. When the drilling fluid reaches the main nozzles cross-section B, the pressure is further reduced to 882,000 Pa, and local turbulence is generated. Subsequently, a part of the drilling fluid moves along the water, and its pressure value is stable at 888,000 Pa. When it reaches outlet C, the pressure increases to 895,000 Pa. At this time, the kinetic energy of the drilling fluid is converted into pressure energy, and a high-pressure area is formed at the bottom hole. When the drilling fluid starts to return after hitting the bottom hole, its pressure decreases continuously and reaches the minimum value of 885,000 Pa at the bottom hole E. This phenomenon is because the hydraulic energy of drilling fluid is converted into kinetic energy after hitting the bottom hole, which decreases the pressure of the drilling fluid and increases the flow rate. The other part of the drilling fluid enters the clearance between the core and the core lifter seat along with A, and the pressure value decreases first and then increases. The above phenomenon is that the clearance A

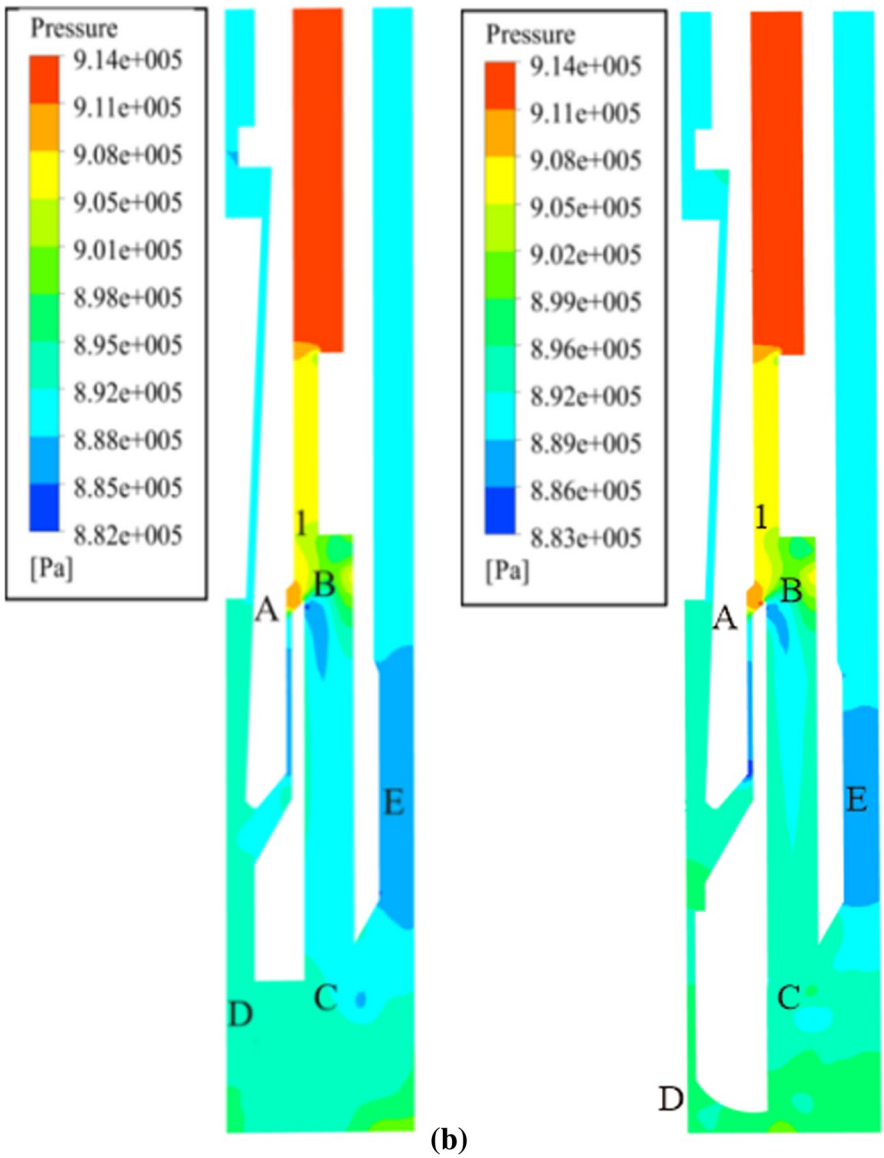

Fig. 8 Pressure contour cross-section of nozzles. **a** Main nozzles cross-section. **b** Assistant nozzles section

between the core, and the core lifter seat is first narrow and then wide, resulting in pressure changes when drilling fluid passes through the clearance.

It can be seen from Fig. 8b that the drilling fluid has the same characteristic trend as the main nozzle at the cross-section of the assistant nozzle, but its outlet pressure at the bottom hole D is higher than that at the main nozzle, and its value is 899,000 Pa. This is mainly due to the different structures of the main nozzle and the assistant nozzle at the waterway, making the diversion at the outlet different after the drilling fluid hits the bottom hole.

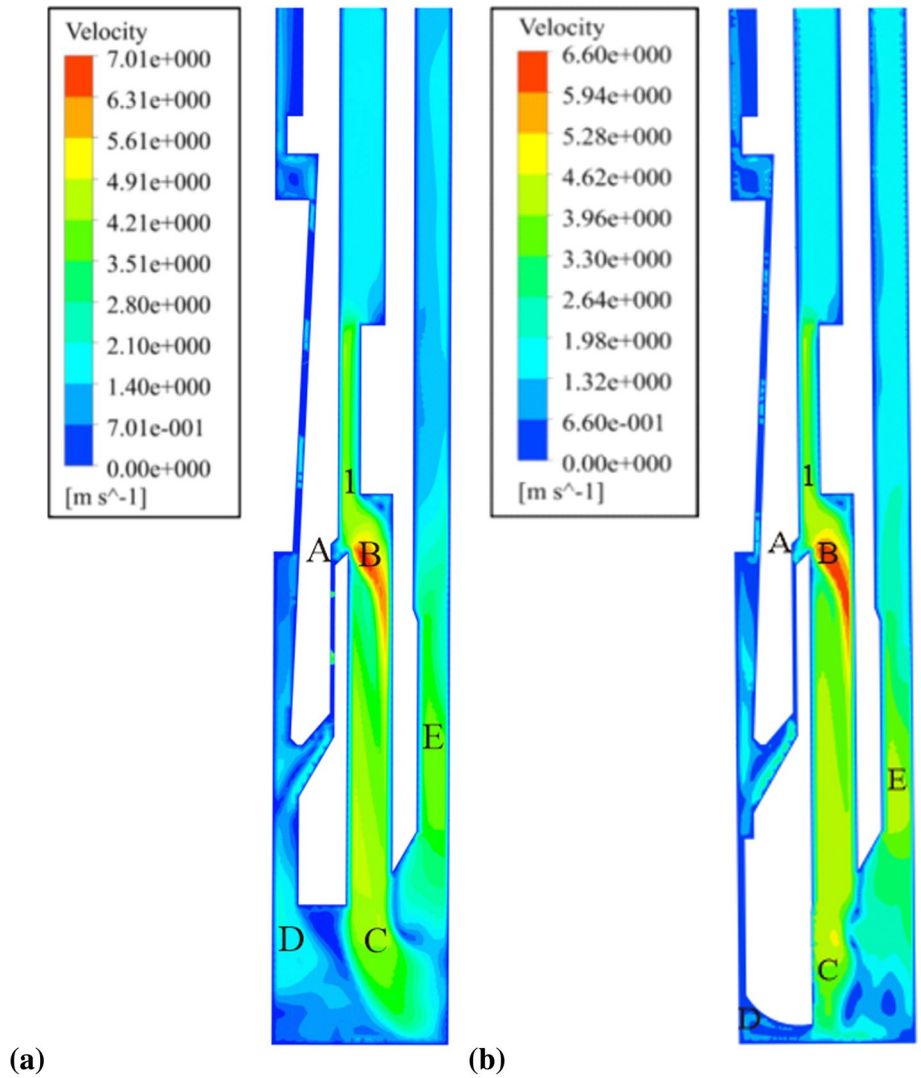

Fig. 9 Velocity contour cross-section of nozzles. **a** Main nozzles section. **b** Assistant nozzles section

Velocity contour analysis of drilling fluid in nozzles cross-section

Figure 9 shows the drilling fluid's velocity contour in the nozzles' cross-section. From Fig. 9a, it can be found that the velocity of drilling fluid reaches 2.8–3.51 m/s when it reaches outlet 1 of the nozzle, and most of it goes down along the nozzle, and a small part goes down along the clearance A between the core lifter seat and the bit. The velocity of drilling fluid along clearance A between the core lifter seat and the bit is only 0.7 m/s. The velocity increases when it reaches the bottom hole D, and its value reaches 1.8 m/s. The reason for the above phenomenon is that the flow rate of drilling fluid along the nozzle is large and the velocity is high, and the value reaches 4.21m/s, while the flow rate of drilling fluid along the clearance A between the core lifter seat and the bit is low and the flow rate is low. Therefore, when the drilling fluid flow along the nozzle passes through the crown of the cutting tooth and the clearance A along the bit, the drilling fluid converges at the bottom hole D, and the velocity increases sharply. Then, the drilling fluid velocity showed a downward trend, reaching

outlet C, the velocity maintained between 3.51 and 4.21m/s. When the drilling fluid flows out of nozzle C and hits the bottom hole, the minimum velocity is 2.1 m/s. At this point, the lower velocity is due to the conversion of drilling fluid kinetic energy into pressure energy. Subsequently, the drilling fluid pressure energy was converted into kinetic energy, and the up-return velocity increased at the bottom hole E, which reached 4.21–4.91 m/s. The increase in the up-return velocity at the bottom hole E is conducive to the smooth passage of cuttings at the bottom hole through the narrow clearance between the drill cutting tooth and the hole wall to avoid the siltation and blockage cuttings. When the drilling fluid passes through E, its up-return velocity gradually tends to be stable and finally remains between 1.4 and 1.8 m/s. This velocity interval meets the normal drilling requirements [7].

It can be found from Fig. 9b that when the drilling fluid reaches region 1 of the assistant nozzles, most of the drilling fluid moves down the nozzle and forms a local high-speed zone, with a speed reaching 6.60 m/s. Different from the velocity contour of the main nozzle, the assistant nozzle has a local low-speed area near the outlet C, in which the outermost layer velocity is 1.98 m/s, the middle layer velocity is 1.32 m/s, and the central area velocity is less than 0.6 m/s. From Fig. 9b, it can also be found that the drilling fluid velocity near the core is only 0.6–0.8 m/s. In addition, it is worth mentioning that the stable return velocity of drilling fluid in the assistant nozzle is slightly higher than that in the main nozzle. It is mainly due to the different outlet structures of the main nozzle and the assistant nozzle, so when the drilling fluid hits the bottom hole, the diversion at the outlet is also different.

Analysis of drilling performance of diamond bit

The designed diamond bit has been verified in geological resource exploration in a sea area of China. The seafloor strata in the target sea area are mainly composed of sediments and non-consolidated quicksand, and there are hard thin flint layers. The drilling equipment adopts the self-developed 60-m multi-purpose seafloor drill. This seafloor drill can carry 25 coring tubes at a time. The operating seawater depth was 900–1200 m. The seawater was used as drilling fluid, and the drilling fluid volume displacement was 62 L/min. The bit pressure was 8–12 kN, the rotary speed was 250–330 rpm. The parameters of the seafloor drill are shown in Table 2.

Table 2 Parameters of the seafloor drill

Overall size	7.6×2.56×2.56 m (H×W×D)
Weight	8.3T
Coring depth	62.5 m
Work water depth	More than 3000 m
Coring modes	Wire line/CPT
Core length	2.5m/barrel
Drilling tool size	HQ
Core diameter	62 mm
Borehole diameter	92 mm

Fig. 10 Field application of diamond bit in seafloor core drilling. 1 Seafloor drill deployment operation, 2 unused diamond bit, and 3 used diamond bit

Table 3 Drilling operation log sheet

Drilling position number	Drill depth/m	Average drilling efficiency m/h	Coring recovery percent %
1	62.5	2.8	86.5
2	62.5	3.1	87.6
3	62.5	3.4	83.2
4	62.5	2.9	90.4
5	62.5	3.3	85.4

The operation process is shown in Fig. 10, and the diamond drilling results are shown in Table 3. The total drilling position was five, cumulative footage was 312.5 m, the average drilling efficiency extends 3m/h, and the average core recovery percent was 86.44%. After drilling, it was found that the diamond edge in the bit matrix was normal, and there was no burning wear in the cutting tooth. The matrix formula, diamond parameters, cutting tooth structure, and water passage system can meet the requirements of seafloor drill operating conditions and marine resource exploration for sample coring quality. It shows that the designed diamond bit can meet the coring target of soft and hard crisscross strata under the seafloor. So the average life of a bit is 180–200 m and is the normal range, and our bit cumulative footage of more than 312 m meets the design requirements.

Conclusions

According to the seafloor drills' working conditions and the complex formation characteristics of the seafloor, this paper aims to improve the adaptability of the diamond bit to the formation and the coring quality. The cutter tooth design scheme of the impregnated diamond

bit is proposed, and Fluent analyzes the flow field of drilling fluid at the bottom hole. Finally, the field drilling test of the diamond bit is carried out, and the conclusions are as follows:

(1) The results of the simulation and seabed test show that the designed bottom-jet diamond bit can effectively avoid the direct erosion of the core by about 85% drilling fluid in the drilling process, and the drilling efficiency is more than 3 m/h, which is conducive to improving the coring rate and drilling efficiency.
(2) The simulation analysis shows that the water passage structure of the bit is reasonable, and the upward return velocity of the drilling fluid can be stabilized between 0.7 and 1.8 m/s, which meets the requirements of the upward return of cuttings in seafloor strata, and has a good hole wall protection performance.
(3) The diamond bit with the main and assistant water channels is designed. The main water channel can play the role of discharging rock powder, and the auxiliary water channel can play the role of assisting the cooling of the bit crown surface.

Abbreviations

HRC	Matrix rockwell hardness
Q	The flow rate of drilling fluid at inlet 2 (L/min)
Q1	The flow rate of drilling fluid at outlet 3 (L/min)
Q2	The flow rate of drilling fluid at outlet 1 (L/min)

Acknowledgements
All authors thank the anonymous reviewers for constructive comments that helped improve this manuscript.

Authors' contributions
JW expounded the theory on which the paper was based, conceived the full-text framework, and carried out engineering tests. CC contributed significantly to the analysis and manuscript preparation. DQ wrote and revised the paper. YS established the simulation model. MY searched for the information and data curation. FP and DP have carried out the drilling testing. The authors read and approved the final manuscript.

Funding
This research is supported by the Hunan Provincial Natural Science Foundation of China (No. 2022JJ30246), Open Research Fund Program of Key Laboratory of Metallogenic Prediction of Nonferrous Metals and Geological Environment Monitoring (Central South University), Ministry of Education (No. 2022YSJS03), National Key R&D Program of China (No. 2017YFC0307501), and Special Project for the Construction of an Innovative Province of Hunan (No.2019GK1012).

Availability of data and materials
All data generated or analyzed during this study are included in this published article.

Declarations

Competing interests
The authors declare that they have no competing interests.

Received: 5 May 2022 Accepted: 22 August 2022
Published online: 15 September 2022

References

1. Agwu OE, Akpabio JU, Alabi SB, Dosunmu A (2018) Artificial intelligence techniques and their applications in drilling fluid engineering: a review. J Pet Sci Eng 167:300–315. https://doi.org/10.1016/j.petrol.2018.04.019
2. Bale AJ, Kenny AJ (2005) Sediment analysis and seabed characterization. Methods Study Mar Benthos 3:43–86
3. Bijay B, George P, Renjith VR, Kurian AJ (2020) Application of dynamic risk analysis in offshore drilling processes. J Loss Prev Proc Ind 68:104326. https://doi.org/10.1016/j.jlp.2020.104326
4. Cao X, Kozhevnykov A, Dreus A, Liu BC (2019) Diamond core drilling process using intermittent flushing mode. Arab J Geosci 12(4):1–7. https://doi.org/10.1007/s12517-019-4287-2
5. Chen Y, Liu ZY, Duan LC (2012) Simulation on hydraulic performance of two kinds of coring diamond bits with different crown. Adv Mat Res 497:350–355. https://doi.org/10.4028/www.scientific.net/AMR.497.350

6. Egede E, Charles E (2021) Common heritage of mankind and the deep seabed area beyond national jurisdiction: past, current, and future prospects. Mar Technol Soc J 55(6):40–52
7. Feng F, Wan BY, Huang XJ (2016) Structure design and optimization of coring bit for soft sea bottom. J Mach Des 33:21–26
8. Franca LFP, Mostofi M, Richard T (2015) Interface laws for impregnated diamond tools for a given state of wear. Int J Rock Mech Min Sci 73:184–193. https://doi.org/10.1016/j.ijrmms.2014.09.010
9. Freudenthal T, Wefer G (2013) Drilling cores on the sea floor with the remote-controlled sea floor drilling rig MeBo. Geosci Instrum Methods Data Syst 2(2):329–337. https://doi.org/10.5194/gi-2-329-2013
10. Gao C, Yuan J (2011) Efficient drilling of holes in Al_2O_3 armor ceramic using impregnated diamond bits. J Mater Process Technol 211(11):1719–1728
11. He S, Peng Y, Jin Y, Wan BY, Liu G (2020) Review and analysis of key techniques in marine sediment sampling. Chin J Mech Eng-En 33(1):1–17. https://doi.org/10.1186/s10033-020-00480-0
12. Jin YP, Wan BY, Liu DS, Peng YD, Guo Y (2016) Dynamic analysis of launch & recovery system of seafloor drill under irregular waves. Ocean Eng 117:321–331
13. Jin YP, Wan BY, Liu DS (2019) Reliability analysis and experimental for key component of launch and recovery equipment of seafloor drill. Chin J Mech Eng 55(08):1–9
14. Meiling J, Jiapin C, Zhiyong O, Lina S, Haixia W, Chun L (2014) Design & application of diamond bit to drilling hard rock in deep borehole. Procedia Eng 73:134–142. https://doi.org/10.1016/j.proeng.2014.06.181
15. Merey Ş (2019) Evaluation of drilling parameters in gas hydrate exploration wells. J Pet Sci Eng 172:855–877. https://doi.org/10.1016/j.petrol.2018.08.079
16. Mostofi M, Richard T, Franca L, Yalamanchi S (2018) Wear response of impregnated diamond bits. Wear 410:34–42. https://doi.org/10.1016/j.wear.2018.04.010
17. Petersen S, Krätschell A, Augustin N, Jamieson J, Hein JR, Hannington MD (2016) News from the seabed–Geological characteristics and resource potential of deep-sea mineral resources. Mar Policy 70:175–187. https://doi.org/10.1016/j.marpol.2016.03.012
18. Piri M, Hashemolhosseini H, Mikaeil R, Ataei M, Baghbanan A (2020) Investigation of wear resistance of drill bits with WC, Diamond-DLC, and TiAlSi coatings with respect to mechanical properties of rock. Int J Refract Met Hard Mater 87:105113. https://doi.org/10.1016/j.ijrmhm.2019.105113
19. Ren YG, Yang L, Liu YJ, Liu BH, Yu KB, Zhang JH (2021) Experimental research on the process parameters of a novel low-load drill bit used for 7000 m bedrock sampling base on manned submersible. J Mar Sci Eng 9(6):682. https://doi.org/10.3390/JMSE9060682
20. Saputra A, Talebi H, Tran D, Birk C, Song C (2017) Automatic image-based stress analysis by the scaled boundary finite element method. Int J Numer Methods Eng 109(5):697-738. https://doi.org/10.1002/nme.5304.
21. Sun W, Gao H, Tan S, Wang Z, Duan LC (2021) Wear detection of WC-Cu based impregnated diamond bit matrix based on SEM image and deep learning. Int J Refract Met Hard Mater 98:105530. https://doi.org/10.1016/J.IJRMHM.2021.105530
22. Sun JH, Li XY, Liu XM, Li XM, Liang J (2016) On drawing up and revising technical requirements of drill rod and casing listed in national standards geo-logical core drilling tool and the implementation. Drilling Eng 5:51–55
23. Sun QB, Shen LN, Yang GS, Tian GL, Ruan HL, Chen X (2020) Design and numerical simulation of multi-layer bit with extra-high matrix. Coal Geol Explor 48:225–230. https://doi.org/10.3969/i.issn.1001-1986.2020.03.032
24. Tan S, Zhang W, Duan L, Pan B, Rabiei M, Li C (2019) Effects of MoS2 and WS2 on the matrix performance of WC based impregnated diamond bit. Tribol Int 131:174–183
25. Wang JL, Qian DL, Sun Y, Peng FF (2021) Design of diamond bits water passage system and simulation of bottom hole fluid are applied to seafloor drill. J Mar Sci Eng 9(10):1100. https://doi.org/10.3390/JMSE9101100
26. Wang J, Yu MF, Qian DL, Wan BY, Sun Y, Chen, Peng DP, Tang YH (2022) Optimisation of drainage performance of the thin-walled core barrel sealing technology for pressure preservation sampling. Ocean Eng 250:110996
27. Wang JL, Zhang SH (2015) A new diamond bit for extra-hard, compact and nonabrasive rock formation. J Cen S Univ 22(4):1456–1462. https://doi.org/10.1007/s11771-015-2663-y
28. Zheng MZ, Li SJ, Yao Z, Zhang AD, Xu DP, Zhou JF (2020) Core discing characteristics and mitigation approach by a novel developed drill bit in deep rocks. J Cen S Univ 27(10):2822–2833. https://doi.org/10.1007/s11771-020-4512-x

Publisher's Note